Int. J. Heat Mass Transfer. Vol. 33, No. 6, pp. 1331–1338, 1990
Printed in Great Britain

0017-9310/90 $3.00+0.00

A numerical analysis of heat transfer and combustion in porous radiant burners

S. B. SATHE, R. E. PECK and T. W. TONG
Department of Mechanical and Aerospace Engineering, Arizona State University, Tempe, AZ 85287-6106, U.S.A.

(*Received* 12 *June* 1989 *and in final form* 12 *September* 1989)

Abstract—A numerical study of combustion and multimode heat transfer in porous radiant burners is performed. Burner characteristics such as flame speeds, radiant outputs and efficiencies are investigated using a one-dimensional conduction, convection, radiation, and premixed flame model. The porous medium is assumed to emit, absorb, and scatter radiant energy. Non-local thermal equilibrium between the solid and gas is accounted for by introducing separate energy equations for the gas and the solid phase. Combustion is described by a one-step global mechanism. The effect of the optical depth, scattering albedo, solid thermal conductivity, upstream environment reflectivity, and interphase heat transfer coupling on the burner performance are studied. It was revealed that for maximizing the radiant output the optical depth should be about ten and the flame should be stabilized near the center of the porous medium. Also, low solid thermal conductivity, low scattering albedo, and high inlet environment reflectivity produced a high radiant efficiency.

INTRODUCTION

A PROMISING development in gas-burner technology is the concept of porous radiant burners (PRB). These devices operate by stabilizing a premixed flame inside or near a non-combustible porous medium. The enthalpy of combustion released in the gas phase heats the porous matrix which then emits thermal radiation to a heat load. In small-scale applications PRB have already shown performance gains over conventional open-flame burners in the form of higher efficiencies, lower NO_x emissions, and more uniform heating [1]. In order to exploit the potential benefits of this technology for the myriad of industrial heating applications, more detailed information about the factors controlling burner performance is needed. The goal of the present work is to provide a better understanding of the link between combustion and heat transfer in PRB and the influence of these processes on the radiant output and burner efficiency.

Recently, Tong and Sathe [2] performed a detailed study of the heat transfer characteristics of PRB. Combustion was represented as a heat generation zone inside the porous medium. It was shown that the properties of the solid matrix such as the thermal conductivity, the optical depth, and the scattering albedo significantly affected the radiative output from the burner. More realistic combustion models were employed by Yoshizawa *et al.* [3] and Chen *et al.* [4] to reveal the structure of radiation-controlled flames in inert porous media. Both studies, however, neglected the important effect of radiation scattering in their analysis and fixed the flame zone at or near the middle of the porous medium. Their results demonstrated the significance of radiative heat transfer in promoting energy feedback ahead of the reaction zone, yielding higher than adiabatic flame speeds. Sathe *et al.* [5] studied numerically the effects of multimode heat transfer and combustion on the flame stability in a finite porous layer. It was shown that stable combustion could be maintained in two different spatial domains. The radiative characteristics of the porous matrix, such as the optical depth and scattering albedo, were also shown to have a considerable effect on flame stability. In some related work DesJardin and Kendall [6] investigated the effect of stoichiometry on the lift-off behavior and radiant output of a radiant surface burner using a simple surface model to account for the radiant heat flux emanating from a porous burner.

The aim of the present study is to investigate the effect of combustion and multimode heat transfer on the radiative output and efficiency of PRB. The study is based on a one-dimensional, premixed methane–air flame model wherein the flame thickness is much thinner than the length of the porous medium. Combustion is modeled using a single-step, irreversible reaction. The solid and gas phases are assumed not to be in local thermal equilibrium. Also, the solid is assumed to emit, absorb, and scatter radiant energy. The computational domain is extended beyond the porous region on either side to accurately model flames close to the edges of the porous region.

MATHEMATICAL ANALYSIS

The schematic diagram of the problem under consideration is shown in Fig. 1. A premixed methane–air gas mixture enters an adiabatic duct containing an inert porous layer of length L. The flame may be

NOMENCLATURE

- a surface area per volume of solid [m^{-1}]
- c specific heat capacity at constant pressure [J kg^{-1} K^{-1}]
- h heat transfer coefficient [W m^{-2} K^{-1}]
- h_k species specific enthalpy [J kg^{-1}]
- i radiant intensity [W m^{-2} sr^{-1}]
- k thermal conductivity [W m^{-1} K^{-1}]
- L porous layer length [m]
- p pressure [N m^{-2}]
- P_1 dimensionless heat transfer coefficient, $haL/\sigma T_i^3$
- P_2 dimensionless thermal conductivity, $k_s/\sigma T_i^3 L$
- q^r radiant heat flux [W m^{-2}]
- q_c reaction enthalpy flux [W m^{-2}]
- Q_c dimensionless enthalpy flux, $q_c/\sigma T_i^4$
- Q^r dimensionless radiant heat flux, $q^r/\sigma T_i^4$
- r reflectivity
- R universal gas constant [J mol^{-1} K^{-1}]
- S dimensionless flame speed, $u(0)/u_{ad}$
- T temperature [K]
- u axial velocity [m s^{-1}]
- V diffusion velocity [m s^{-1}]
- W molecular weight [kg mol^{-1}]
- $\bar{W}$ average molecular weight [kg mol^{-1}]
- x axial coordinate [m]
- Y mass fraction.

Greek symbols

- ε emissivity
- η_o output radiative efficiency, $q^r(L)/q_c$
- η_t total radiative efficiency, $\{q^r(L)-q^r(0)\}/q_c$
- θ dimensionless temperature, $(T-T_i)/T_i$
- μ direction cosine in equation (5)
- ξ dimensionless axial coordinate, x/L
- ρ gas density [kg m^{-3}]
- σ Stefan–Boltzmann constant [W m^{-2} K^{-4}]
- σ_a, σ_s, σ_e absorption, scattering and extinction coefficients [m^{-1}]
- τ optical depth, $\sigma_e L$
- ϕ porosity
- $\dot{\omega}$ molar generation rate [mol m^{-3} s^{-1}]
- ω scattering albedo, σ_s/σ_e.

Superscripts

- + positive direction
- − negative direction
- r radiation.

Subscripts

- a apparent
- ad adiabatic
- b black body
- c combustion
- d diffuse, downstream
- e exit plane
- g gas
- i inlet plane
- k index for species
- s solid
- u upstream.

located either inside or outside the porous layer and the flame thickness is much less than L. The flow is assumed to be one-dimensional, steady, and laminar. The viscous effects are neglected so that the momentum equation can be integrated and replaced by the condition that the thermodynamic pressure is a constant, which is the case for most PRB. The solid matrix is assumed to be gray and to emit, absorb, and scatter radiant energy. Gaseous radiation is neglected compared to solid radiation. Non-local thermal equilibrium between the gas and the solid phase is accounted for by considering separate energy equations for the two phases. All the properties of the solid are assumed to be homogeneous and constant.

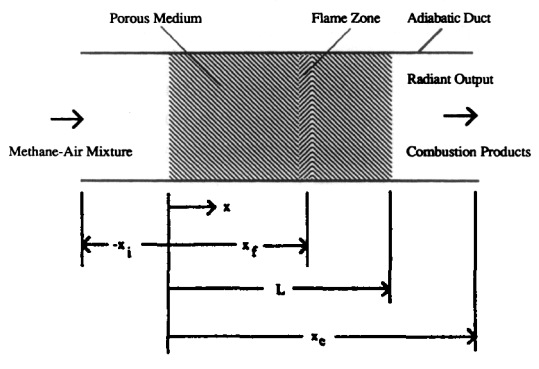

FIG. 1. Schematic diagram of the porous radiant burner.

The methane–air combustion is modeled using the one-step global reaction [7] for an equivalence ratio of one so that the only species involved are CH_4, O_2, N_2, CO_2 and H_2O. The reaction rate constant is given by $k_c = 1.8 \times 10^8 \exp(-125\,600/RT_g)$ [CH_4] mol m^{-3} s^{-1}. The thermodynamic and transport properties of the gases are evaluated using the CHEMKIN [8] and TRANFIT [9] codes, respectively, from Sandia National Laboratory.

The governing equations are written by incorporating convection, conduction, radiation, and combustion mechanisms. A more detailed description of the heat transfer model may be found in Tong and Sathe [2]. The governing equations are then:

Continuity equation

$$\frac{d}{dx}(\rho u \phi) = 0 \tag{1}$$

where ϕ is the porosity so that $\phi < 1$ for $0 < x < L$ and $\phi = 1$ elsewhere. All the symbols are identified in the Nomenclature.

Species conservation equation

$$\rho u\phi \frac{dY_k}{dx} + \frac{d}{dx}(\rho\phi Y_k V_k) = \phi\dot{\omega}_k W_k \quad (k = 1, K) \quad (2)$$

where the diffusion velocity V_k is the sum of the diffusion velocities due to mole fraction gradients and thermal gradients [10].

Gas energy equation

$$\rho u\phi c_g \frac{dT_g}{dx} + (1-\phi)ha(T_g - T_s) + \phi \sum_{k=1}^{K} \rho Y_k V_k c_k \frac{dT_g}{dx} = -\phi \sum_{k=1}^{K} \dot{\omega}_k h_k W_k + \frac{d}{dx}\left(\phi k_g \frac{dT_g}{dx}\right). \quad (3)$$

Solid energy conservation

$$\frac{d}{dx}\left[(1-\phi)k_s \frac{dT_s}{dx}\right] + (1-\phi)ha(T_g - T_s) = \frac{dq^r}{dx}. \quad (4)$$

Radiative transfer equation (RTE)

$$\mu \frac{\partial i(x,\mu)}{\partial x} + (\sigma_a + \sigma_s) i(x,\mu) = \sigma_a i_b(T_s) + \frac{\sigma_s}{2}\int_{-1}^{1} i(x,\mu')\, d\mu' \quad (5)$$

where μ' is the dummy variable of integration.

Equation of state

$$\rho = \frac{\bar{W}p}{RT_g}. \quad (6)$$

Boundary conditions

The gas temperature and the species concentrations are specified at the inlet section ($x = -x_i$), whereas vanishing gradients are imposed at the exhaust section ($x = x_e$)

$$Y_k = Y_{k,i}, \quad T_g = T_i \quad \text{at} \quad x = -x_i$$

$$\frac{dY_k}{dx} = \frac{dT_g}{dx} = 0 \quad \text{at} \quad x = x_e. \quad (7)$$

The boundary conditions for the solid temperature are written assuming that the solid loses heat convectively to the gas [2] so that

$$-k_s \frac{dT_s}{dx} = h(T_g - T_s) \quad \text{at} \quad x = 0$$

$$k_s \frac{dT_s}{dx} = h(T_g - T_s) \quad \text{at} \quad x = L. \quad (8)$$

The upstream boundary condition for the radiant intensity is written assuming that the upstream environment can be characterized by a gray diffusely emitting and reflecting surface. On the downstream side, the burner is assumed to be seeing a black environment at $T_b = 298$ K. Thus, we have

$$i^+(0) = \varepsilon i_b(T_i) + 2r_d \int_0^1 i^-(0, -\mu')\mu'\, d\mu' \quad \text{at} \quad x = 0$$

$$i^-(L) = i_b(T_b) \quad \text{at} \quad x = L. \quad (9)$$

The radiative heat flux appearing in the solid energy equation is given by

$$q^r = 2\pi \int_{-1}^{1} i(x,\mu')\mu'\, d\mu'. \quad (10)$$

Upon nondimensionalizing the above equations, the dimensionless quantities relevant to this study are: $\xi = x/L$, $\theta = (T - T_i)/T_i$, $P_1 = haL/\sigma T_i^3$, $P_2 = k_s/\sigma T_i^3 L$, $\omega = \sigma_s/\sigma_e$, and $\tau = \sigma_e L$ where $\sigma_e = \sigma_a + \sigma_s$. The symbols are described in the Nomenclature.

Solution procedure

The radiative transfer equation (RTE) was transformed into a set of ordinary differential equations using the spherical harmonics approximation, and Marshak's formulation was used to model the boundary conditions [11, 12]. The reader is referred to these references for the details on the spherical harmonic method. An efficient numerical scheme was devised to solve the governing equations by modifying PREMIX [10]. The PREMIX code has been applied successfully to solve the governing equations pertaining to flame propagation in premixed gaseous systems. The code employs finite-difference techniques with adaptive gridding and solves the set of non-linear governing equations by the damped Newton–Raphson method. The principal modification to the code was the addition of the solid energy equation and the differential equations resulting from the spherical harmonic approximation for the RTE. As noted earlier, the computational domain was extended on both the upstream and downstream sides of the porous layer in order to accurately model flames situated close to the edge of the porous medium. The flame location was fixed numerically by setting the gas temperature at a particular point in the domain, and the governing equations were then solved so that the flame speed was an eigenvalue. A word should be added about the spherical harmonics approximation. Considerable convergence difficulties were observed when the order of the spherical harmonics method was increased and only results for the P-3 approximation could be obtained. Nevertheless, a separate study using the earlier code [2] revealed that for optical thicknesses greater than or equal to one, the difference in the radiative outputs obtained by the P-3 and P-11 approximations was less than 1%.

The governing equations were solved using the IBM 3090 computer. The time required to solve for one set

of parameters ranged widely from approximately 100–500 CPU seconds, depending on the initial guess provided. Since the Newton–Raphson method was used, very good initial guesses were required to obtain convergence, otherwise divergence resulted. A relative convergence criterion of 10^{-4} was specified for Newton's iteration. Computations were continued on successively finer grids until the flame speed changed by no more than 0.1%. An overall energy balance of approximately 0.5% was achieved for most of the cases, with an energy balance of less than 1% in the worst case. Approximately 100 grid points were required. Reducing the grid refinement criterion had a negligible effect on the results but required more computer time. Also, care was taken to keep the computational domain large enough so that flame speed was not affected by the length of the computational domain [13]. The accuracy of the numerical code was checked by comparing the results with the laminar flame speed and adiabatic flame temperature data of Reitz and Bracco [7] by letting the porosity be close to one.

RESULTS AND DISCUSSION

The above model is used to calculate results for a wide range of properties of the porous layer that may be encountered in PRB. In particular, the effect of the extinction coefficient (σ_e), scattering coefficient (σ_s), solid thermal conductivity (k_s), heat transfer coupling (ha), and the upstream environment reflectivity (r_d) on the flame speeds, radiant outputs, and radiant efficiencies are investigated. The porous layer is assumed to be 5 cm long and have a porosity (ϕ) of 0.95. A stoichiometric fuel–air mixture is allowed to enter the duct with a uniform velocity and inlet temperature, $T_i = 298$ K. Variations were made in the following baseline property values to produce the results presented below: $\sigma_e = 20\ \mathrm{m}^{-1}$, $\sigma_s = 10\ \mathrm{m}^{-1}$, $k_s = 10\ \mathrm{W\,m^{-1}\,K^{-1}}$, $ha = 2.0 \times 10^9\ \mathrm{W\,m^{-3}\,K^{-1}}$, and $r_d = 0$. The thermal conductivity of the solid, k_s, was intended to be that for non-metallic solids, such as alumina and silica employed in PRB. The value of ha was estimated using the experimental data for h for cylinders in cross-flow and a was computed assuming infinitely long fibers of 10 μm diameter [2]. The corresponding relevant non-dimensional parameters are: $\tau = 1$, $\omega = 0.5$, $P_1 = 6.67 \times 10^7$, $P_2 = 133.3$.

Figure 2 presents the computed burning velocities for different flame locations, ξ_f, obtained by varying the extinction coefficient ($\sigma_e = \sigma_a + \sigma_s$) from 20 to 200 m^{-1} so that the total optical thickness of the layer ($\tau = \sigma_e L$) ranges from 1.0 to 10.0 while the scattering albedo ($\omega = \sigma_s/\sigma_e$) is kept constant at 0.5. The flame location is defined as the position where the reaction rate is a maximum. The upstream (inlet) and downstream (outlet) edges of the porous medium are denoted by vertical dashed lines at $\xi = 0$ and 1, respectively. The flame speeds are normalized by the adiabatic flame speed which prevails a few millimeters

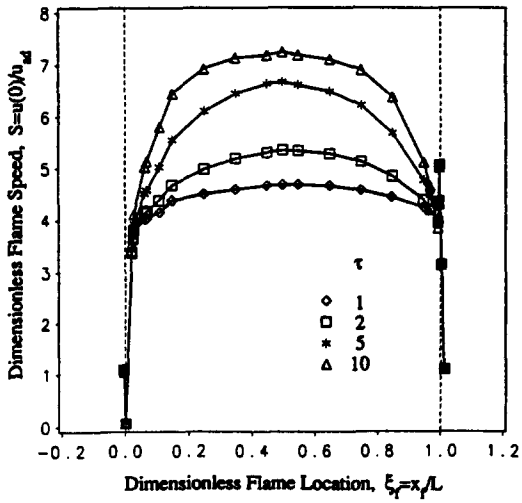

FIG. 2. Effect of the burner optical thickness on the flame speed for different flame locations.

beyond either side of the porous layer. It was revealed in an earlier study [5] that the flame speed variation near the edge of the porous medium is controlled by conduction, whereas radiation heat transfer becomes a contributing factor for flame propagation in the interior. A higher thermal conductivity on the upstream side of the flame results in a preferential conductive heat transfer in the upstream direction, thereby increasing the flame speed, such as at the downstream edge of the porous medium. An opposite effect occurs at the upstream edge. When the flame approaches the porous medium from the downstream side, the flame speed increases abruptly because of the higher thermal conductivity encountered in the preheat zone until a local maximum is observed at the edge of the porous medium. As the flame enters the porous region the burning velocity is reduced, mainly because the upstream conductive heat flux is diminished as the downstream side of the flame is being replaced by higher conducting material. The radiation heat loss in the downstream direction accounts for the local minimum in flame speed that is lower for higher optical depths, but the effect is much smaller than for the heat conduction. As the flame is shifted toward the center of the porous region, the lengthening amount of material radiating in the post-flame zone directs the radiation upstream causing the flame temperature and speed to increase. Beyond the symmetry axis this radiant energy feedback escapes across the inlet plane producing lower flame speeds. A broad maximum in the flame speed near the center of the porous layer was also observed by Yoshizawa *et al.* [3]. As the flame approaches the upstream edge, the flame speed drops drastically due to increased radiative loss and the preferential distribution of the conductive flux in the downstream direction due to greater resistance to upstream conduction. The flame at the upstream edge is characterized by a very broad flame zone of the order of centimeters and it is anticipated that such a

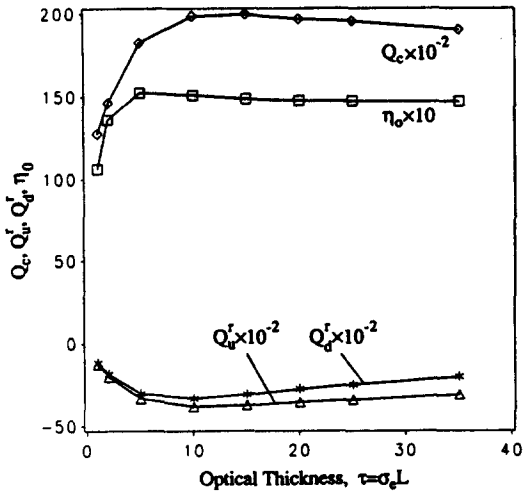

FIG. 3. Effect of the optical depth on the radiation feedback, flame speed, and radiative output efficiency for $x_f/L = 0.5$.

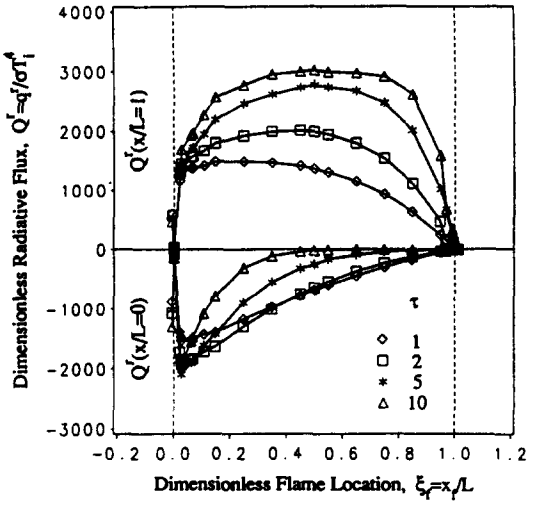

FIG. 4. Radiant output (downstream radiative flux) and upstream radiative flux for varying optical thicknesses and flame locations.

flame is not physically plausible [5]. After this minimum the flame speed returns to the adiabatic value as there is no radiation loss from the flame and the conductivity value is that of the fuel–air mixture. The fact that the flame speeds at the downstream edge of the porous medium are unchanged by the optical thickness provides further evidence that the thermal conductivity is the controlling parameter for the burning rate at this location. Because the flame location is important from the standpoint of radiant energy exchange and determining the maximum allowable heat release, it should be emphasized that only those portions of the velocity profile with positive slope would be expected to maintain stable combustion.

The effect of the optical thickness on combustion–heat transfer behavior deep in the porous region is illustrated in Fig. 3. It is evident that the reactant enthalpy flux Q_c (proportional to the flame speed) increases as τ is increased from 1 to about 10 due to enhanced radiation feedback across the flame in the upstream direction. This explanation is substantiated by the radiative energy fluxes at the upstream and downstream edges of the flame zone. The quantities Q_u^r and Q_d^r in the figure are the radiant fluxes on the upstream and downstream edges of the flame zone respectively. The edge of the flame zone is taken to be the location where the reaction rate is 1/1000 of its peak value. However, as τ is increased further beyond 10, the diminishing radiative energy feedback across the flame zone lowers the reactant enthalpy flux. This trend is consistent with results obtained by Chen *et al.* [4]. The output radiative efficiency, defined as the ratio of the radiant output (radiant heat flux at $\xi = x/L = 1$) and the reactant enthalpy flux, reaches a maximum at about $\tau \approx 5$ and then decreases very gradually.

The upstream and downstream radiative fluxes (at $\xi = x/L = 0$ and 1, respectively) resulting from different flame locations and optical thicknesses are shown in Fig. 4. The upstream and downstream radiative fluxes depend on the heat generation rate, which is proportional to the flame speed, and the optical depths between the flame and the edges of the porous medium. For a fixed τ the upstream radiative flux increases as the flame moves upstream from the outlet plane due to an increase in flame speed and because there is less shielding between the flame and the upstream edge. The heat flux continues to increase due to the reduced shielding until the sharp drop in flame speed near the inlet occurs. When the flame is near the downstream edge, the shielding effect dominates, so that the upstream radiative flux is higher for lower τ. However, when the flame is outside the porous layer and near the upstream edge, there is no shielding effect involved and the upstream radiant flux is largest for the largest τ due to greater emission. Similarly, the downstream radiative flux increases when the flame is moved upstream due to an increase in the flame speed and an increase in the extent of porous material at elevated temperatures. Thus, for the flames situated very close to the downstream edge the radiative flux is almost zero because for $\sigma_e = 200\ \mathrm{m}^{-1}$, the optical thickness is of the order of 0.01; hence, the radiative output is negligible. As the flame shifts inwards the burning velocity drops by about 13.5% from its peak value at the interface due to the redistribution of the conductive heat flux; however, because the optical thickness of the high-temperature region increases by about 700%, no corresponding decrease in the radiative output is observed. Beyond this point the radiative output keeps rising due to the elongating high-temperature zone in conjunction with the increase in flame speed up to the middle of the porous burner section. As the flame moves further upstream, the radiative output decreases eventually because the reduction in flame speed and shielding on the downstream side outweighs the increase in the

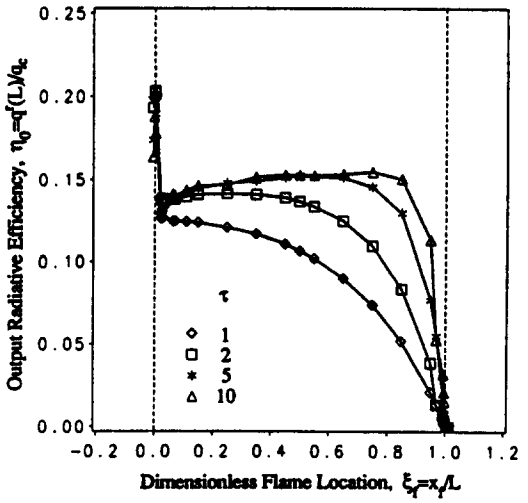

FIG. 5. Variation of the radiative output efficiencies for different optical thicknesses and flame locations.

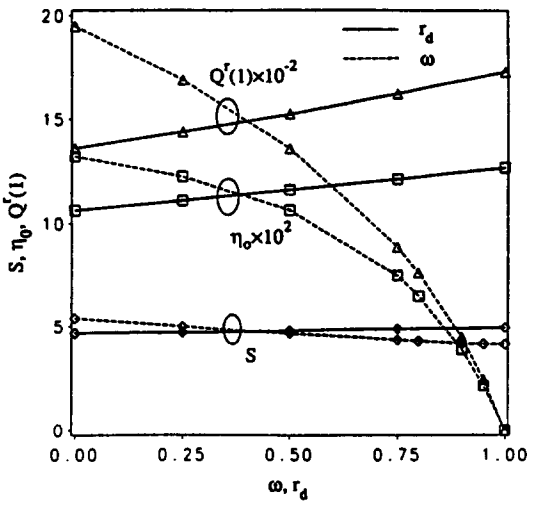

FIG. 6. Burner characteristics for different scattering albedos and upstream reflectivities when $x_f/L = 0.5$.

amount of high-temperature porous material. The shielding effect is more important for larger optical thicknesses; hence, the peak in the radiant output occurs at more downstream positions. For the flame located upstream of the porous region, due to the shielding effect, the radiant output is larger for a smaller τ. These results are consistent with those of Tong and Sathe [2] where the peak in the radiant output shifted downstream with increasing τ even when the flow speed was held constant.

The radiative output efficiencies for different flame locations and optical depths are shown in Fig. 5. The efficiencies are nearly zero when the flames are at the outlet plane and increase quickly at higher τ to values ranging from 12 to 15% as the flame is moved upstream. It is interesting to note that the highest efficiencies are achieved when the flame is located outside the porous medium near the upstream edge and that the efficiency at this position increases with decreasing optical depth. However, from the recent study of Sathe *et al.* [5] the flame outside the porous layer near the upstream edge is unstable since the slope of the curve of flame speed versus distance is negative. A negligible increase in efficiencies is observed in the upstream half (which is the stable flame region) of the porous material when τ is increased above 5. These findings suggest that to maximize both the radiant output and efficiency the flame should be located at the center of the porous material, but the maximum radiant output occurs when $\tau \approx 10$ and the maximum radiant output efficiency occurs when $\tau \approx 5$.

Figure 6 shows the effect of the upstream environment (at $\xi = -x_i/L = -\xi_i$) reflectivity and the scattering albedo on the burner characteristics for a flame located at $x_f/L = 0.5$ when the downstream environment is black. A reduction in albedo increases the flame speed due to stronger emission from the solid. It must be noted that when there is no emission or absorption by the solid, i.e. when $\omega = 1$, the flame speed exceeds the adiabatic value because the thermal conductivity of the solid matrix is much greater than that of the gas. Both the radiant output and the efficiency also increase with a decrease in the albedo; hence, a strongly emitting–absorbing medium is preferred to enhance the burner performance. The results demonstrate that for the conditions investigated scattering by the solid is an important mechanism in the radiative transport and cannot be neglected. Results for flame locations other than at the center of the solid indicated similar trends when the albedo was varied and are not shown here. An increase in the upstream diffuse reflectivity reduces the radiation loss from the flame in the upstream direction, thereby raising the flame temperature and accelerating the flame speed. The radiant output increases when the reflectivity is increased because the flame speeds are higher and less radiation escapes in the upstream direction. This latter effect also improves the output efficiency and suggests that a large reflectivity is desired for the best burner performance. These results are consistent with the findings of Tong and Sathe [2].

The burner characteristics for different thermal conductivities of the solid are shown in Fig. 7. An increase in the thermal conductivity increases the flame speed due to an enhancement in the preheating of the incoming reactants. However, the increase in the solid conductivity does not increase the radiant output to the same extent as the flame speed so that the radiative efficiency actually declines. This result is due to the fact that for the same flow rates and heat release rate, an increase in the solid conductivity produces lower post-flame temperatures and higher pre-flame temperatures, thereby reducing the radiative output [2]. Thus, the radiant output can be increased by increasing the conductivity and concurrently sacrificing on the radiant efficiency.

The effect of the heat transfer coupling between the

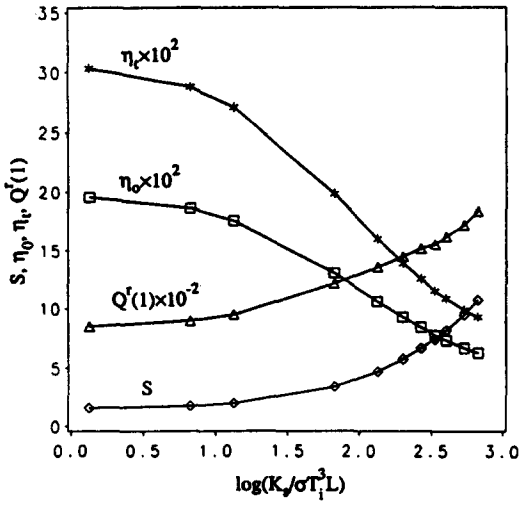

FIG. 7. Effect of the solid thermal conductivity on the burner characteristics when $x_f/L = 0.5$.

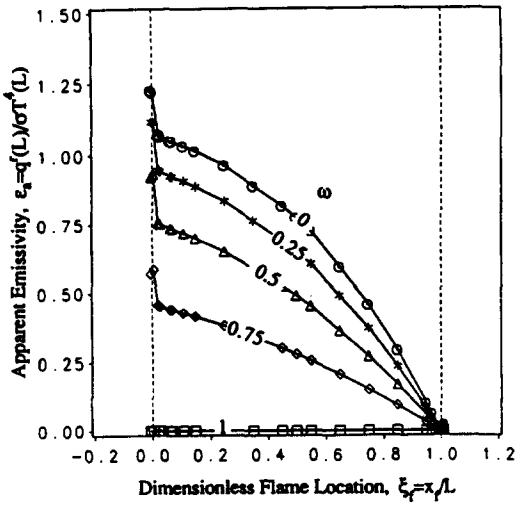

FIG. 9. Apparent emissivity of the burner for different scattering albedos.

solid and the gas is reported in Fig. 8. A stronger heat transfer coupling results in a better pre-heating effect when the solid conductivity is higher than that of the gas. Hence, the flame speed increases as the heat transfer coupling is increased. Once the coupling is large enough so that the gas and solid are in local thermal equilibrium, i.e. $P_1 \geqslant 8 \times 10^7$, the rise in flame speed becomes negligible. On the other hand, when the heat transfer coupling is weak, very little energy is transferred from the gas to the solid so that the flame speed approaches the adiabatic flame speed. This asymptotic approach to the adiabatic flame speed has served as an additional check of the code. The radiative output increases as the heat transfer coupling is enhanced because of higher solid temperatures, and no appreciable increase occurs once the solid and gas have reached thermal equilibrium. The radiant efficiency is observed to pass through a maximum as the heat transfer coupling is enhanced.

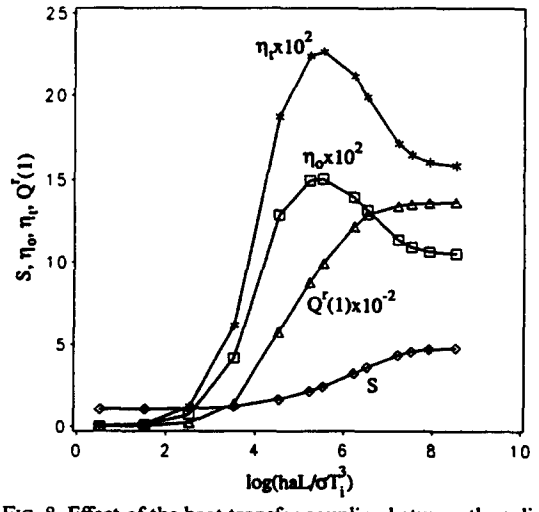

FIG. 8. Effect of the heat transfer coupling between the solid and the gas on the burner characteristics when $x_f/L = 0.5$.

The apparent emissivity of the burner, defined as $\varepsilon_a = q^r/\sigma T^4$ at $\xi = 1$, is shown in Fig. 9. An attempt is being made in the industrial sector to characterize the emissivity of the porous burner as a gauge of its performance [6]. It is seen that as the porous medium becomes strongly emitting and absorbing (albedo becomes smaller), the apparent emissivity increases. This result is due to the fact that as albedo decreases q^r increases, whereas the temperature rise is not appreciable. The apparent emissivity is also a strong function of the flame location. Thus, a unique value of this quantity cannot be assigned to a particular burner unless the exact flame location for a given firing rate is known.

CONCLUSIONS

The effect of combustion and multimode heat transfer on the performance characteristics of PRB has been studied numerically. The model incorporated emission, absorption, and scattering of radiant energy by the porous matrix and accounted for non-local thermal equilibrium between the gas and solid phases. The computational domain was extended on either side of the porous medium to accurately model the flames located near the edge of the porous medium. It was revealed that for maximizing the radiant output, the optical depth should be approximately ten with the flame located near the center of the porous medium, and the heat transfer coupling should be high enough to ensure local thermal equilibrium between the gas and the solid. The solid phase conduction and scattering had a significant effect on the burner performance. Low solid conductivities and scattering albedos are desirable to increase the radiant efficiency.

Acknowledgement—The authors gratefully acknowledge the support of this research provided by the Office of Basic Energy Sciences, U.S. Department of Energy, under contract number DE-FG02-87ER13697.

REFERENCES

1. *Gas Research Institute Digest* 7, July/August (1984).
2. T. W. Tong and S. B. Sathe, Heat transfer characteristics of porous radiant burners, *ASME Publication HTD* **104**, 147–155 (1988).
3. Y. Yoshizawa, K. Sasaki and R. Echigo, Analytical study of the structure of radiation controlled flame, *Int. J. Heat Mass Transfer* 31, 311–319 (1988).
4. Y.-K. Chen, R. D. Matthews and J. R. Howell, The effect of radiation on the structure of premixed flame within a highly porous inert medium, *ASME Publication HTD* 81, 35–42 (1987).
5. S. B. Sathe, R. E. Peck and T. W. Tong, Flame stabilization and multimode heat transfer in inert porous media : a numerical study, *Combust. Sci. Technol.* 70, 93 (1990).
6. S. T. DesJardin and R. M. Kendall, Fundamental studies of flame attachment on radiant surface burners, Paper No. WSCI87-81, Western States Section/The Combustion Institute Meeting, Honolulu, Hawaii (1987).
7. R. D. Reitz and F. V. Bracco, Toward the formulation of a global–local equilibrium kinetics model for laminar hydrocarbon flames. In *Numerical Methods in Laminar Flame Propagation* (Edited by N. Peters and J. Warnatź), pp. 130–151. Vieweg (1982).
8. R. J. Kee, J. A. Miller and T. H. Jefferson, CHEMKIN : a general-purpose problem-independent, transportable, Fortran chemical kinetics code package, Sandia National Laboratories Report SAND80-8003 (1980).
9. R. J. Kee, G. Dixon-Lewis, J. Warnatz, M. E. Coltrin and J. A. Miller, A Fortran computer code package for the evaluation of gas-phase multicomponent transport properties, Sandia National Laboratories Report SAND86-8246 (1986).
10. R. J. Kee, J. F. Grcar, M. D. Smooke and J. A. Miller, A Fortran program for modeling steady laminar one-dimensional premixed flames, Sandia National Laboratories Report SAND85-8240 (1985).
11. B. Davison and J. Sykes, *Neutron Transport Theory*. Oxford University Press, London (1957).
12. M. N. Ozisik, *Radiative Heat Transfer and Interactions with Conduction and Convection*. Wiley–Interscience, New York (1973).
13. M. D. Smooke, J. A. Miller and R. J. Kee, Determination of adiabatic flame speeds by boundary value methods, *Combust. Sci. Technol.* 34, 79–90 (1983).

ANALYSE NUMERIQUE DU TRANSFERT THERMIQUE ET DE LA COMBUSTION DANS LES BRULEURS POREUX RADIANTS

Résumé—Une étude numérique est faite sur la combustion et le transfert thermique multimode dans des brûleurs poreux radiants. Des caractéristiques de brûleur telles que vitesse de flamme, rayonnement et efficacité sont étudiées à partir d'un modèle monodimensionnel de conduction, convection, rayonnement et prémélange. Le milieu poreux est supposé émettre, absorber et diffuser l'énergie radiative. Le non-équilibre thermodynamique local entre le solide et le gaz est pris en compte en introduisant des équations d'énergie séparées pour les phases solide et liquide. La combustion est décrite par un mécanisme global à un échelon. L'effet sur les performances du brûleur de l'épaisseur optique est étudié ainsi que l'albédo, la conductivité thermique du solide, la réflectivité de l'environnement, le couplage de transfert thermique à l'interface. Pour augmenter au maximum la puissance radiante, l'épaisseur optique doit être de l'ordre de dix et la flamme doit être stabilisée près du centre du milieu poreux. Et aussi une faible conductivité thermique du solide, un faible albédo et une réflectivité élevée de l'environnement produisent une efficacité radiante élevée.

EINE NUMERISCHE ANALYSE DER WÄRMEÜBERTRAGUNG UND VERBRENNUNG IN PORÖSEN STRAHLUNGSBRENNERN

Zusammenfassung—Die Verbrennung und die unterschiedlichen Wärmeübertragungsmechanismen in porösen Strahlungsbrennern werden numerisch untersucht. Dabei werden unter Verwendung eindimensionaler Wärmeleitung, Konvektion, Strahlung und eines Flammenmodells mit Vormischung typische Brennereigenschaften wie Flammengeschwindigkeit, Strahlungsleistung und Wirkungsgrad betrachtet. Es wird vorausgesetzt, daß das poröse Medium Strahlungsenergie emittiert, absorbiert und streut. Das nichtlokale thermische Gleichgewicht zwischen Festkörper und Gas wird dadurch berücksichtigt, daß getrennte Energiegleichungen für das Gas und den Festkörper eingeführt werden. Die Verbrennung wird durch einen globalen Einstufenmechanismus beschrieben. Die Einflüsse der optischen Dicke, des Anteils der Streureflexion, der Feststoffwärmeleitfähigkeit, das Reflexionsvermögen der stromaufwärts-gelegenen Umgebung und der Wärmeübergang zwischen den Phasen werden in Abhängigkeit von der Brennerleistung untersucht. Es zeigt sich, daß für eine Maximierung der Strahlungsleistung die optische Dicke ungefähr zehn betragen sollte und die Flamme in der Nähe des Zentrums des porösen Mediums stabilisiert werden sollte. Geringe Feststoffwärmeleitfähigkeit, ein geringer Anteil der Streureflexion und hohe Umgebungsreflexion am Eintritt produzieren ebenfalls eine hohe Strahlungseffizienz.

ЧИСЛЕННЫЙ АНАЛИЗ ТЕПЛОПЕРЕНОСА И ГОРЕНИЯ В ПОРИСТЫХ РАДИАЦИОННЫХ ГОРЕЛКАХ

Аннотация—Численно исследуются горение и многорежимный теплоперенос в пористой радиационной горелке. С использованием одномерной модели теплопроводности, конвекции, радиации и предварительно смешанного пламени изучаются такие характеристики горелки, как скорость пламени, излучаемая мощность и коэффициент полезного действия источника излучения. Предполагается, что пористая среда испускает, поглощает и рассеивает энергию излучения. Нелокальное тепловое равновесие между твердым телом и газом учитывается по отдельности уравнениями энергии для газовой твердой фазы. Процесс горения описывается при помощи одноступенчатого глобального механизма. Исследуется влияние оптической глубины, альбедо рассеяния, коэффициента теплопроводности твердого тела, отражательной способности окружающей среды вверх по течению, а также связи теплопереноса на межфазной границе на рабочие характеристики горелки. Показано, что выделение энергии становится максимальным при оптической глубине, равной приблизительно десяти, а также при стабилизации пламени вблизи центра пористой среды. Высокий коэффициент полезного действия источника излучения достигается при низкой теплопроводности твердого тела, низком альбедо рассеяния и высокой отражательной способности окружающей среды.